Supplementary Material: Action of the general anaesthetic isoflurane reveals coupling between viscoelasticity and electrophysiological activity in individual neurons

Casey Adam,[1,2*] Celine Kayal,[1,2] Ari Ercole,[3] Sonia Contera,[4*]
Hua Ye,[1,2] Antoine Jerusalem[1*]

[1]Department of Engineering Science, University of Oxford,
Parks Road, Oxford, OX1 3JP, UK
[2]Institute of Biomedical Engineering, University of Oxford
Old Road Campus, Roosevelt Drive, Oxford, OX3 7DQ, UK
[3]Division of Anaesthesia, University of Cambridge
Addenbrooke's Hospital, Cambridge, CB2 0QQ, UK
[4]Department of Physics, University of Oxford
Parks Road, Oxford, OX1 3PU, UK

[*]To whom correspondence should be addressed;
adamc@purdue.edu, sonia.antoranzcontera@physics.ox.ac.uk, antoine.jerusalem@eng.ox.ac.uk

Supplementary Material

1 Supplementary Note 1: Nanoindenter working principle

In order to calculate force F, force amplitude F_0, indentation depth h, and indentation amplitude h_0 during nanoindenter measurements, the following formulas are applied.[1] Note that the formula for F, equation (S2), is Hooke's law.[1]

$$h = d_p - d \tag{S1}$$

$$F = -kd \tag{S2}$$

Here, k is the cantilever's spring constant, d_p is the displacement (in nm) of the piezoelectric chip controlling the cantilever's proximity to the sample, and d is the cantilever displacement.[1] Both k and d_p are known because k is calibrated by the cantilever manufacturer and d_p is the piezo extension/contraction in nanometers.[2] To calculate d_p, the voltage, V_p, applied to make the piezo expand or contract is multiplied by a constant C, in nm/V.[2] C is calibrated when the piezo is manufactured.[2] Throughout an experiment, d is measured via interferometry as follows.[3–5]

In interferometry, an IR laser with a wavelength $\lambda = 1{,}550$ nm[2] is delivered from a source through a fiberoptic cable, where laser light then exits the cable, passes through the experimental medium (in this case, FluoroBrite DMEM imaging media, ThermoFisher, A1896701), hits the tip of the cantilever, then reflects back into the cable, where the laser is then detected by a photodiode.[3–5] The distance between the end of the optical fiber and the cantilever is ℓ, meaning that the optical path length is 2ℓ.[3–5] The photodiode reads a wave that arises from light reflected at the fiber-medium interface and light reflected from the cantilever.[3–5] When the cantilever is out of contact with the sample, destructive interference occurs between both waves, and little to no signal reaches the photodiode.[4,5] When in-contact with a sample, tip/sample interaction

forces cause the cantilever to bend, thereby changing ℓ, and the signal passing into the detector is no longer cancelled.[4,5] The signal on the photodiode is therefore dependent on ℓ, which in turn is dependent on d.[4,5]

The photodiode signal and ℓ are related as follows.[3–5]

$$V(\ell) = \frac{V_{\text{max}} + V_{\text{min}}}{2}\left[1 + \left(\frac{V_{\text{max}} - V_{\text{min}}}{V_{\text{max}} + V_{\text{min}}}\right)\cos\left(\frac{4\pi\ell}{\lambda} + \varphi_0\right)\right] \tag{S3}$$

Here, φ_0 is a constant phase shift that depends only on the geometry of the cantilever, V_{max} represents the voltage on the photodiode at maximum interference, and V_{min} represents the photodiode voltage at minimum interference.[3] For small changes in ℓ, typically the case in cell DMA, the photodiode reading is close to the quadrature point, defined as the midpoint of the interference signal, and equation (S3) can be linearised as follows.[3–5]

$$V(\ell) = \frac{V_{\text{max}} + V_{\text{min}}}{2}\left[1 + \left(\frac{V_{\text{max}} - V_{\text{min}}}{V_{\text{max}} + V_{\text{min}}}\right)\left(\frac{4\pi\ell}{\lambda}\right)\right] \tag{S4}$$

Assuming that changes in ℓ are solely due to changes in d, and neglecting changes in λ due to the medium, the following expression can be used to calculate cantilever deflection at any given moment.[3,4]

$$d = \Delta\ell = \left[\frac{\lambda}{2\pi\left(V_{\text{max}} - V_{\text{min}}\right)}\right]\Delta V \tag{S5}$$

Note that d is converted from photodiode readings to nanometers via multiplication by a calibration factor obtained during initial probe calibration before cell measurements are collected.[2]

2 Supplementary Note 2: Calcium imaging analysis algorithm

The effect of isoflurane on neuron firing activity was analysed via calcium imaging. As described in Materials and Methods, six calcium imaging movies, each with a duration of 3 min and a frame rate of 400 ms, were collected during a single experiment: one before isoflurane exposure, three during isoflurane exposure (at time points of 15 min, 30 min, and 45 min of

exposure), and two after isoflurane exposure (at time points of 30 min and 45 min after exposure stopped). Analysis of these calcium imaging movies was performed via a custom script in MATLAB R2019a. For any given movie, the script identified cells, obtained a fluorescence time trace for each individual cell in the movie frame, and identified and counted spikes in the time trace that corresponded to firing events from the cell. This process was repeated for all six movies in the given experiment. The script also tracked cells between movies, in order to determine if each given cell altered firing activity between experimental time points. The script outputs the number of times each individual cell fired during all six movies from a single calcium imaging experiment. All cell identification, tracking, and spike counts were validated by eye.

2.1 Identifying individual cells

The following procedure was used to threshold cells from background. First, a 2D image of the cells was generated by summing the fluorescence intensity (FI) of each pixel through all movie frames. This 2D image was then de-noised by applying MATLAB's built-in *wiener2* function twice and the contrast enhanced via MATLAB's built-in *adapthisteq* function. Next, any cells on the boarder of the movie frame were removed from analysis via MATLAB's built-in *imclearborder* function. Otsu's method, MATLAB's *multithresh* function, was then applied to threshold out pixels belonging to cells. Holes in the binary images were then filled, and edges smoothened via MATLAB's built-in *imfill*, *imopen*, and *bwareaopen* functions.

After thresholding cells from background, a unique ID was assigned to each cell in the movie frame via cell segmentation. First, the 2D image generated by summing the FI of all movie frames was eroded and reconstructed as disks by applying MATLAB's built-in *strel*, *imerode*, and *imreconstruct* functions. This step was necessary to ensure correct cell segmentation. Next, *watershed* was applied to the complement of the reconstructed image to segment

the cells and assign each a unique ID.

2.2 Tracking cells between calcium imaging movies

If the movie being analysed was not the first movie of the experiment (i.e., the movie being analysed belonged to the During or After time points), the ID of any given cell generated from *watershed* for the current movie was altered to match that assigned to the same cell in the previous movie. In this manner, cells were assigned only one ID throughout an experiment (e.g., cell 117 was labelled cell 117 in all six movies).

Since the F11 cells used in these experiments were not migratory, cell tracking was accomplished by comparing cell coordinates between two movies as follows. The spatial coordinates of a cell in the current movie were compared to the ID assigned to the same spatial position in the previous movie. If a cell ID had been assigned in the previous movie, the cell ID in the current movie was reassigned to match. If a cell ID had not been assigned in the previous movie, the cell was given a new ID. If multiple cell IDs registered for the cell's spatial coordinates (for example, a cluster of cells that moved relative to one another), the maximum ID number was assigned to the cell in the current movie.

Occasionally, a frame shift occurred between movies within a single experiment. Therefore, it was necessary to identify whether such a shift occurred. To do so, the algorithm used the 2D image (constructed by summing the FI of each pixel in all movie frames) of the movie being analysed as well as that of the movie from the previous time point. Feature detection and tracking between each image was performed using MATLAB's built-in *detectBRISKFeatures*, *extractFeatures*, and *matchFeatures* functions. Frame shifts were then detected and calculated by taking the difference between feature coordinates (MATLAB's *matchFeatures* function) between images. If a frame shift occurred, shifted cell coordinates in the current movie were compared to cell coordinates in the previous movie. Otherwise, direct cell coordinate compar-

isons were made. Any cells that were not in the frame of the previous movie (e.g., as the result of a frame shift or of migration) were assigned a new ID.

2.3 Counting the number of times a given cell fired

Once cell IDs were assigned, time traces (TTs) were generated by summing the FI of all pixels belonging to a particular cell (with a unique ID) for each movie frame. Spikes in the TT that correspond to firing events were then detected and counted as follows. The algorithm determined whether the cell fired at all during the TT by looking at the spread of the data, which was larger and less-symmetric for cells that fired. Specifically, it was unlikely that the cell fired during the movie if $\sqrt{\max(\mathrm{TT}) - \mathrm{median}(\mathrm{TT})}/\mathrm{median}(\mathrm{TT}) \leq 0.005$. The threshold of 0.005 was chosen by trial and error, and validated by eye. If a firing event occurred in the TT, the number of spikes (firing events) was counted as follows. First, the TT was smoothed, detrended, and normalised via MATLAB's built-in *smooth*, *detrend*, and *wiener2* functions. To further distinguish TT spikes, the time derivative of the TT was taken via MATLAB's *gradient* function. Finally, spikes were detected and counted by identifying peaks in the time derivative greater than a certain threshold. The threshold value was determined via Otsu's method (MATLAB's *multithresh* function). The firing count for each TT was validated by eye, and manually corrected if the user disagreed with the algorithm.

3 Supplementary Note 3: Alterations in neuron activation and inactivation

Cell (in)activation was analysed in order to examine whether isoflurane affected neuronal firing patterns and investigate why cells appeared to compensate for isoflurane after exposure to the anaesthetic for 45 min. Activation occurred if a cell did not fire in the previous time point, but fired in the current time point. Inactivation occurred if a cell did not fire in the current time

point, but had fired in the previous time point. Reactivation occurred if a cell activated again after at least one inactivation, and is therefore a subset of the cells that activate at a particular time point.

Cell activation and inactivation did not vary significantly between treatments, as shown in Supplementary Figure S6 and Supplementary Tables S8 and S9. However, as shown in Supplementary Figure S7(a) and Supplementary Table S5, significantly more cells reactivated during 45 min of isoflurane exposure ($p = 0.04$, unpaired t-test, details in Supplementary Table S5) and 45 min after isoflurane exposure ($p = 0.02$, unpaired t-test, details in Supplementary Table S5) compared to the flowing air control. Additionally, as shown in Supplementary Figure S7(b), the mean amount of time that passed before a cell reactivated was significantly shorter ($p \leq 0.05$, unpaired t-tests) for cells exposed to isoflurane compared to both controls. These observations support the hypothesis that cells compensate for the presence of isoflurane and reactivate as isoflurane exposure persists. While reactivation significantly varied between treatments (unpaired t-tests, details in Supplementary Table S5), reactivation did not significantly vary through time within a given treatment (unpaired t-tests, details in Supplementary Table S10).

In spite of the fact that activation and inactivation did not significantly vary between each treatment (Supplementary Figure S6 and Supplementary Tables S8 and S9), the pattern of cell activation and inactivation through time was affected by treatment. As shown in Supplementary Table S6, for cells exposed to isoflurane, more cells activated at 45 min during isoflurane exposure, compared to 30 min of isoflurane exposure ($p = 0.03$, unpaired t-test, details in Supplementary Table S6). This observation coincides with the hypothesis that cells compensate for the presence of isoflurane between the 30 and 45 min measurements. As shown in Supplementary Table S7, fewer cells inactivated between 15 min and 30 min of exposure to isoflurane ($p = 0.03$, unpaired t-test, details in Supplementary Table S7), and again between 30 min and 45 min of isoflurane exposure ($p = 0.03$, unpaired t-test, details in Supplementary Table S7). Therefore,

as neurons were exposed to isoflurane for longer times, fewer neurons inactivated. Once isoflurane exposure stopped, and cells were allowed to recover for 30 min, the number of cells that inactivated increased ($p = 0.05$, unpaired t-test, details in Supplementary Table S7). Together, these observations demonstrate that if a cell becomes active during exposure to isoflurane, the neuron is more likely to remain firing until isoflurane is removed from the system.

As shown in Supplementary Tables S6 and S7, there was no significant change in activation or inactivation for cells exposed to flowing air (test details in each table). For no flow control cells, more cells activated 75 min into the experiment, i.e., for the equivalent of the 30 min After time point ($p = 0.05$, unpaired t-test, details in Supplementary Table S6). This observation corresponds to the fact that a few outlier cells, indicated by arrows in Supplementary Figure S5, began firing at this time point. Inactivation significantly increased ($p = 0.04$, unpaired t-test, details in Supplementary Table S7) in the final experimental time point. This observation corresponds to a general inactivation of cells at the end of the experiment, already discussed in the results from figure 2(b) and shown in Supplementary Figure S5.

4 Supplementary Figures

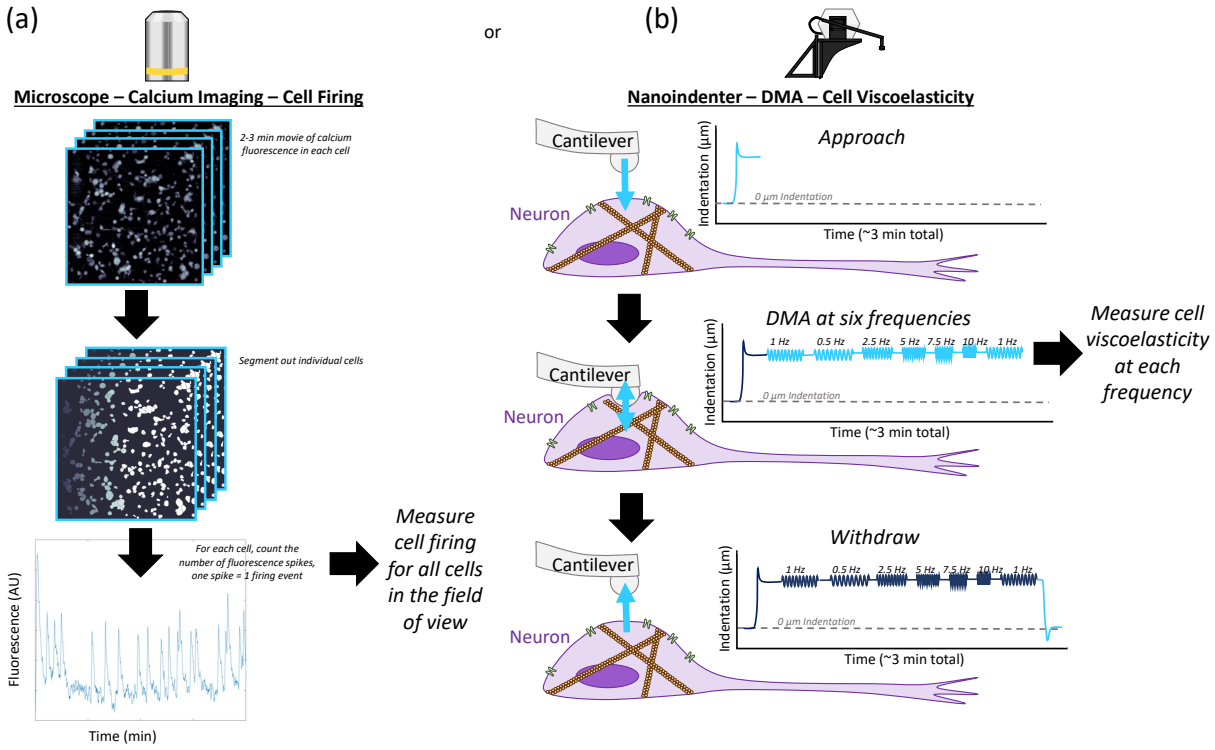

Figure S1: Measurement procedure schematic. At various time points during isoflurane exposure, cell firing (a) or viscoelasticity (b) were measured. As shown in (a), cell firing was measured by calcium imaging. In calcium imaging, a sudden increase in the fluorescence intensity of a cell indicates a firing event. To count firing events for each cell within the field of view, a 2-3 min movie of cell fluorescence was recorded with a frame rate of 400 ms. Individual cells were then identified and segmented. The fluorescence intensity of each cell was summed for each frame of the movie, resulting in fluorescence vs. time plots for each cell (bottom image). Fluorescence spikes corresponding to firing events were then counted for each cell. As shown in (b), viscoelasticity was measured by dynamic mechanical analysis (DMA). A single neuron was indented with a spherical tip attached to a cantilever. After indenting to an initial depth of a few microns (approach), DMA at 1 Hz, 0.5 Hz, 2.5 Hz, 5 Hz, 7.5 Hz, 10 Hz, and 1 Hz was performed. Cell viscoelasticity was calculated from cantilever deflection, see equations 1-3, at each frequency. The 1 Hz measurement was repeated in order to ensure that the cell had not suffered damage during the measurements. After DMA, the cantilever was withdrawn from the cell until the next experimental time point.

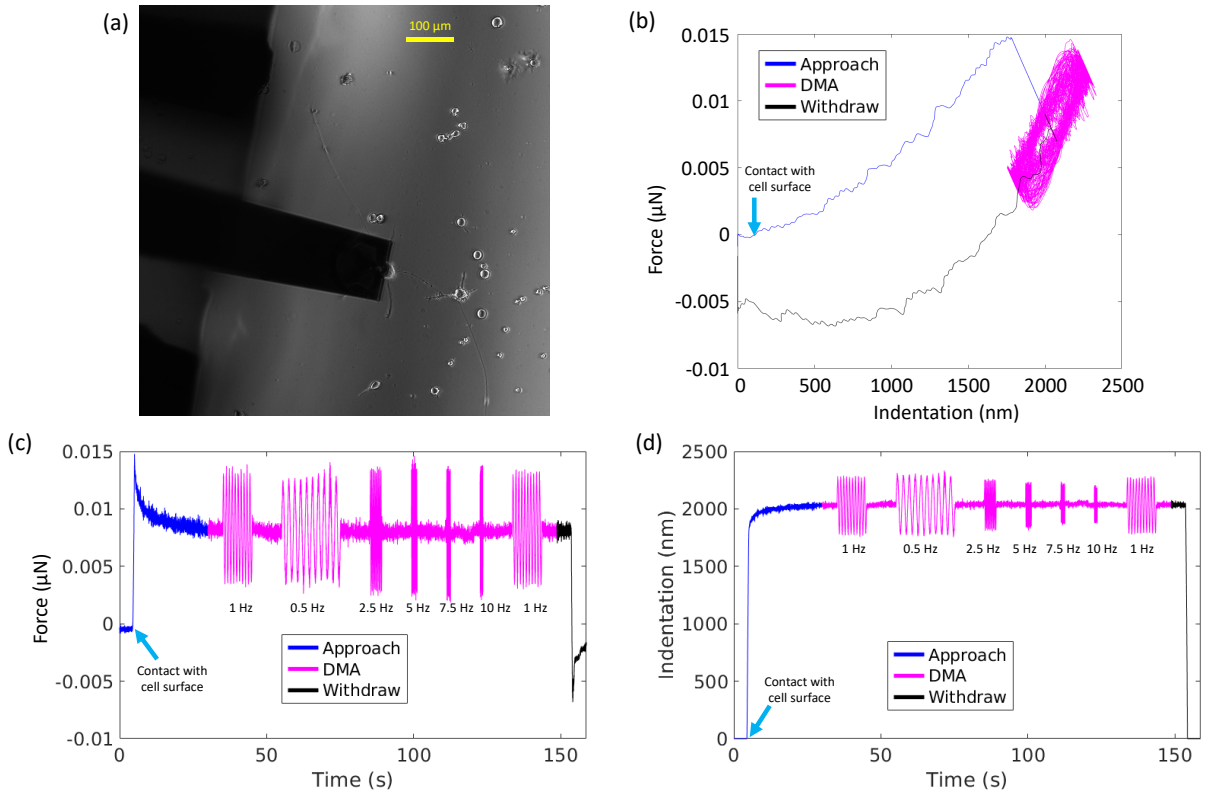

Figure S2: Example raw dynamic mechanical analysis (DMA) data. Microscale DMA was performed to measure neuron viscoelasticity. In microscale DMA, a spherical tip attached to a cantilever applies an oscillatory stimulus to a sample. Cantilever deflection as the tip interacts with the sample is used to calculate sample indentation depth (equation S1) and the force experienced by the cantilever (equation S2). Sample viscoelasticity is calculated from the force and indentation during the applied DMA oscillations via equations 1-3. An optical image of a neuron and cantilever during DMA is shown in (a). A representative force vs. indentation curve from a single DMA measurement is shown in (b): as the cantilever approaches and indents the cell (blue), DMA is performed (magenta), and the cantilever is withdrawn (black). The force (c) and indentation (d) experienced by the cell through time are also shown, along with each DMA frequency. Blue arrows indicate the contact point, where the tip first comes into contact with the cell surface.

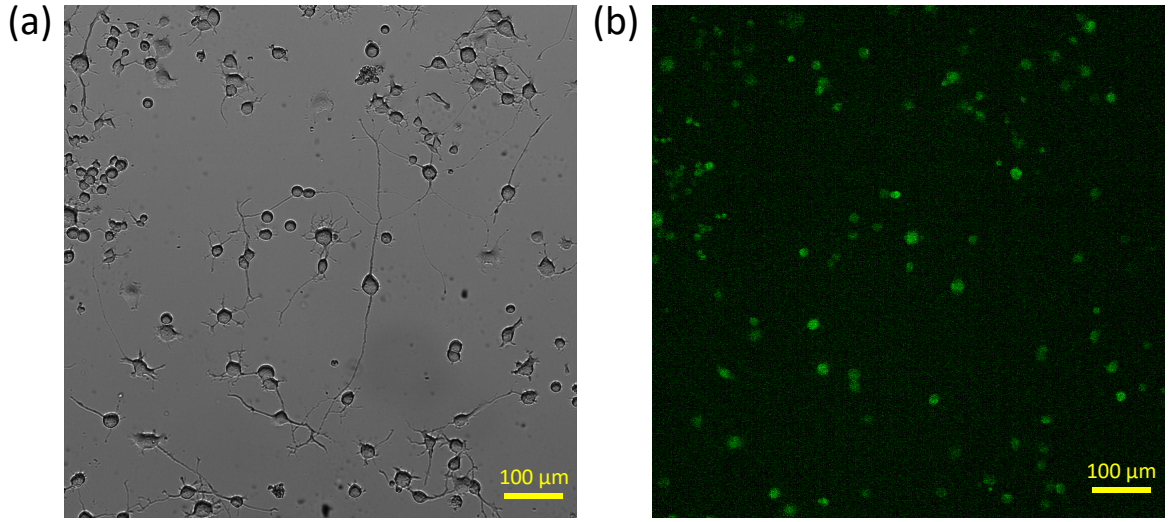

Figure S3: Example raw calcium imaging data. In calcium imaging, cells are exposed to Oregon Green BAPTA dye, which fluoresces in the presence of calcium. Sudden increases in Oregon Green BAPTA fluorescence, called spikes, indicate firing events as firing causes a sudden release of calcium into the cytoplasm. To detect spikes, Oregon Green BAPTA fluorescence is recorded in a 2-3 min movie. A sample brightfield image of neurons is shown in (a). The corresponding Oregon Green BAPTA fluorescence, collected with a 400 ms exposure time, is shown in (b). While the small exposure time decreases the fluorescence signal to noise ratio, the 400 ms exposure increases the time resolution of the movie and reduces the likelihood of dye photobleaching.

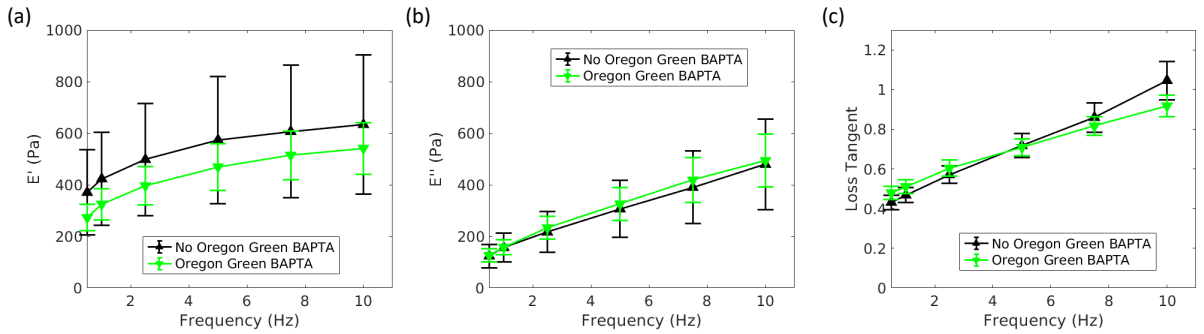

Figure S4: Effect of Oregon Green BAPTA on cell mechanics. Oregon Green BAPTA, the fluorescent dye used in calcium imaging, diffuses throughout the neuronal cytoplasm, and thereby has the potential to alter cell viscoelasticity. Neuronal storage moduli (E'), loss moduli (E''), and loss tangents ($\tan\delta$) when the dye is present in the cytoplasm (green triangles pointing down), and when the dye is not present (black triangles pointing up) are shown in (a)-(c), respectively. Points and error bars respectively represent the mean and standard error of measurements from 12 neurons with and 12 neurons without the dye. Cell viscoelasticity is not significantly altered by the dye (p-values and test details are provided in Supplementary Table S1).

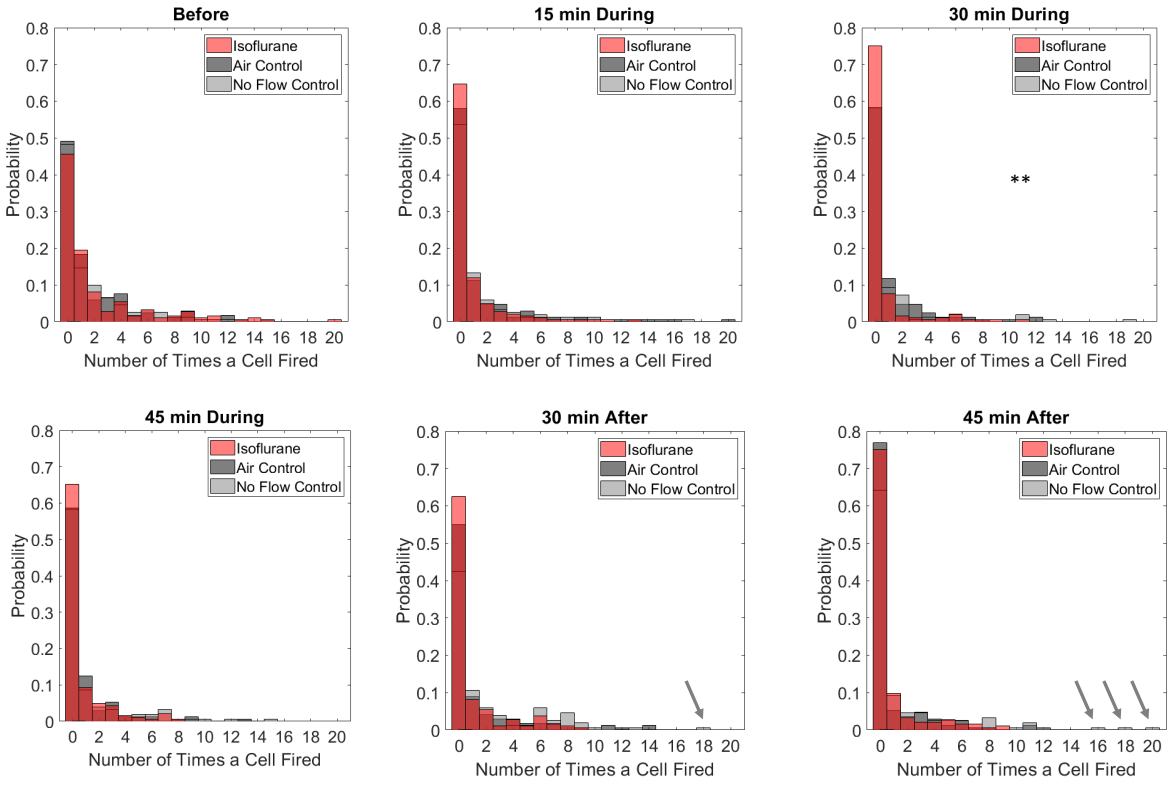

Figure S5: Histograms of the number of times neurons fired at each experimental time point. Probability distributions for the firing counts of cells exposed to isoflurane, flowing air, and no flow are shown in red, black, and grey, respectively. A double asterisk indicates that isoflurane was significantly different from both controls ($p \leq 0.0043$, Wilcoxon rank sum test, all p-values and test details are provided in Supplementary Table S3). Grey arrows indicate outlier cells with a large number of firing events which contribute to the increase in no flow control cell firing during the last two experimental time points ($p \leq 0.014$, Wilcoxon rank sum test, all p-values and test details are provided in Supplementary Table S3).

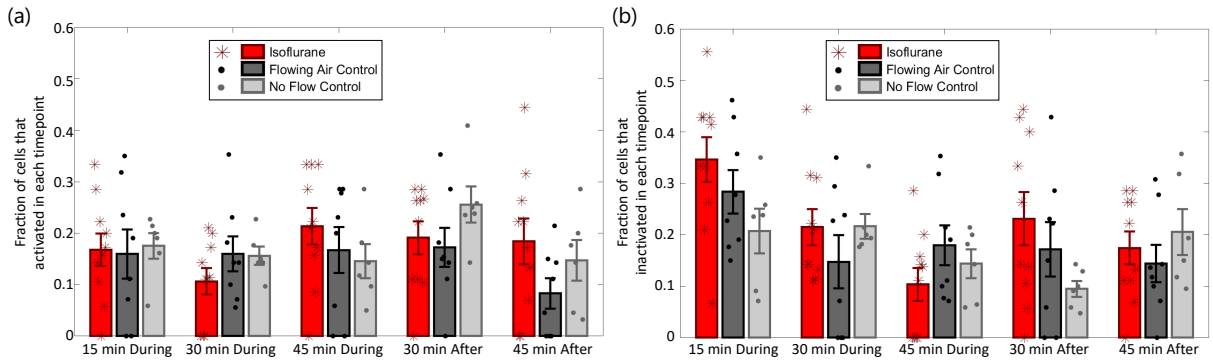

Figure S6: Neuron activation and inactivation at different experimental time points. The time points when activation and inactivation could be observed occur at 15, 30, and 45 min during exposure to isoflurane, flowing air, or air without gas flow, as well as 30 and 45 min after exposure. The fraction of cells that activated, calculated as the number of cells that activated at a particular time point divided by the number of cells that fired during the experiment is shown in (a). The fraction of cells that inactivated, calculated as the number of cells that inactivated at a particular time point divided by the number of cells that fired during the experiment is shown in (b). Asterisks and points represent individual biological replicates for isoflurane (red asterisks), flowing air control (black dots), and no flow control (grey dots) samples. There is no significant difference in activation and inactivation between the three treatments. Test p-values and details are provided in Supplementary Table S8 and S9 for (a) and (b), respectively. All error bars represent the standard error.

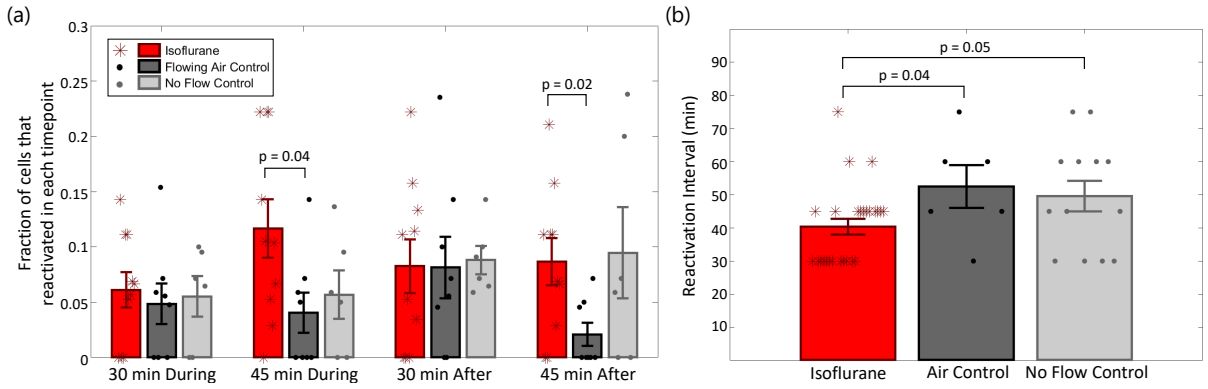

Figure S7: Effect of isoflurane on neuron reactivation. Panel (a) shows the fraction of cells that reactivated, calculated as the number of cells that reactivated during a particular time point divided by the number of cells that fired during the experiment. Time points when reactivation can be observed are 30 and 45 min During exposure to isoflurane (red), flowing air (black), or air without gas flow (grey), as well as 30 and 45 min After. Asterisks and points represent individual biological replicates. Panel (b) shows the mean reactivation interval, the amount of time that passed before a cell reactivated. Asterisks and points represent individual neurons that reactivated during the experiment. Significant differences between treatments are indicated with p-values calculated from unpaired t-tests. All p-values and test details can be found in Supplementary Table S5 for panel (a), and are shown in panel (b). Error bars represent the standard error.

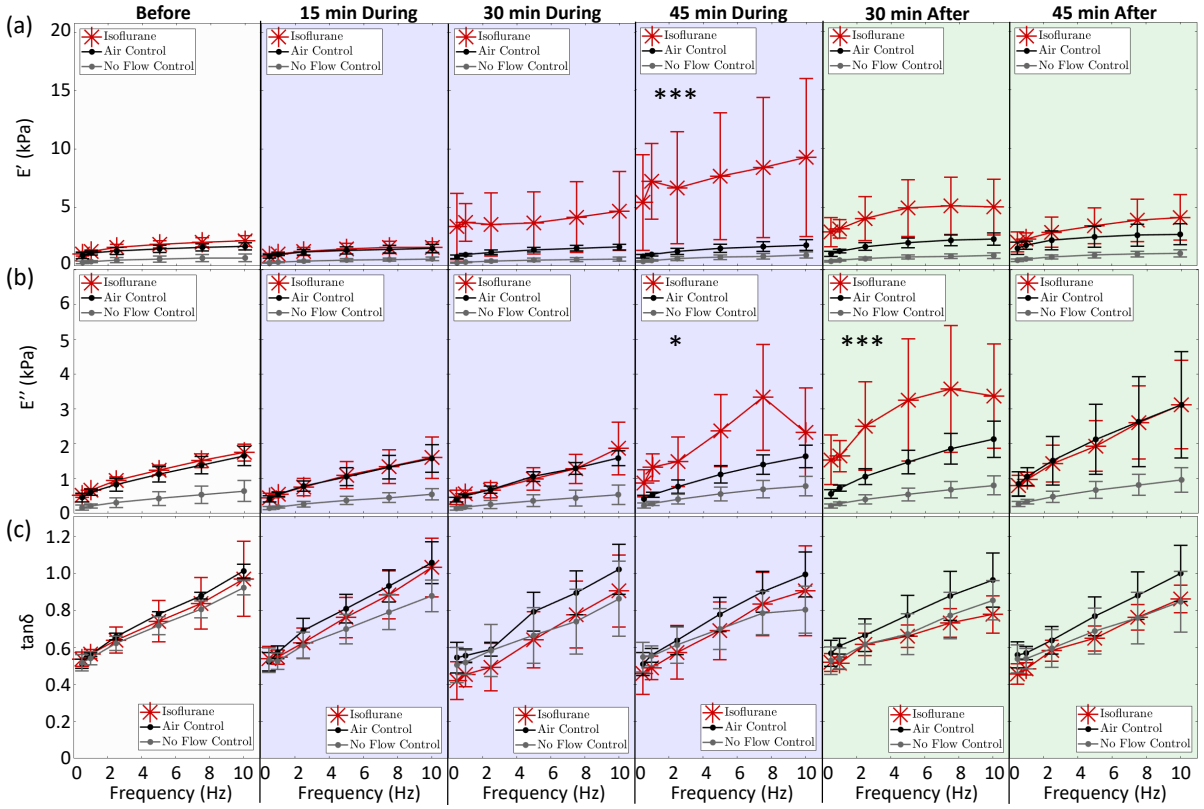

Figure S8: Dynamic mechanical analysis of cells exposed to isoflurane. Neurons were exposed to a flow of 1% anaesthetic isoflurane gas (red asterisk), a flow of compressed air (air control, black dots), or no gas flow (no flow control, grey dots). Dynamic mechanical analysis was performed on individual cells before gas flow (Before), at 15 min intervals during gas exposure (blue shading, 15 min During, 30 min During, and 45 min During), and at specific time points after gas exposure (green shading, 30 min After and 45 min After). The mean storage modulus E' (Pa), loss modulus E'' (Pa), and loss tangent $\tan\delta = E''/E'$ throughout the course of the experiment are shown in (a)-(c), respectively. Error bars represent the standard error. Significant differences between isoflurane and both control treatments, calculated by *post hoc* comparisons using Tukey's honest difference criterion (all p-values and details are provided in Supplementary Table S12), are indicated by a single black asterisk * for $p < 0.05$, or three black asterisk *** for $p < 0.0001$.

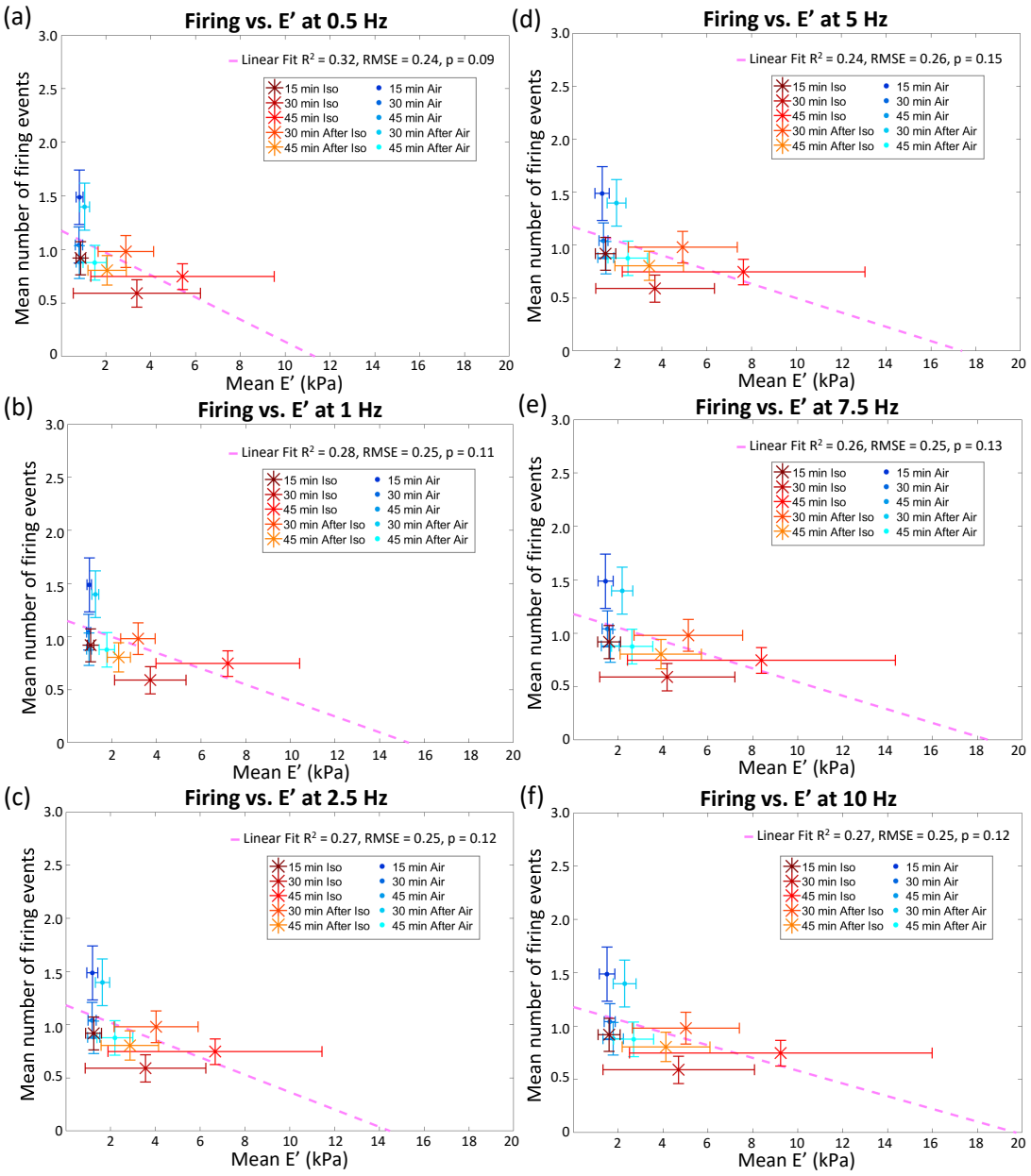

Figure S9: Correlation between neuronal firing and storage modulus. Neurons were treated with isoflurane (iso, red/yellow asterisk), or flowing air (air, blue/cyan points) as a control to determine effects caused by isoflurane. Linear regression (pink dashed lines, metrics shown in each panel and in Supplementary Table S14) was performed on the mean number of times neurons fired vs. mean neuronal storage modulus (E') measured at: 0.5, 1, 2.5, 5, 7.5, or 10 Hz, shown in (a)-(f), respectively. Linear regression was performed on measurements collected at five experimental time points: 15, 30, and 45 min during gas exposure, and 30 and 45 min after gas exposure (indicated by point shading). Measurements before gas exposure were excluded because the sample was at a higher temperature during Before measurements than during subsequent measurements. Similarly, control measurements of no gas flow were excluded from the regression in order to avoid convoluting the effects of isoflurane with gas flow.

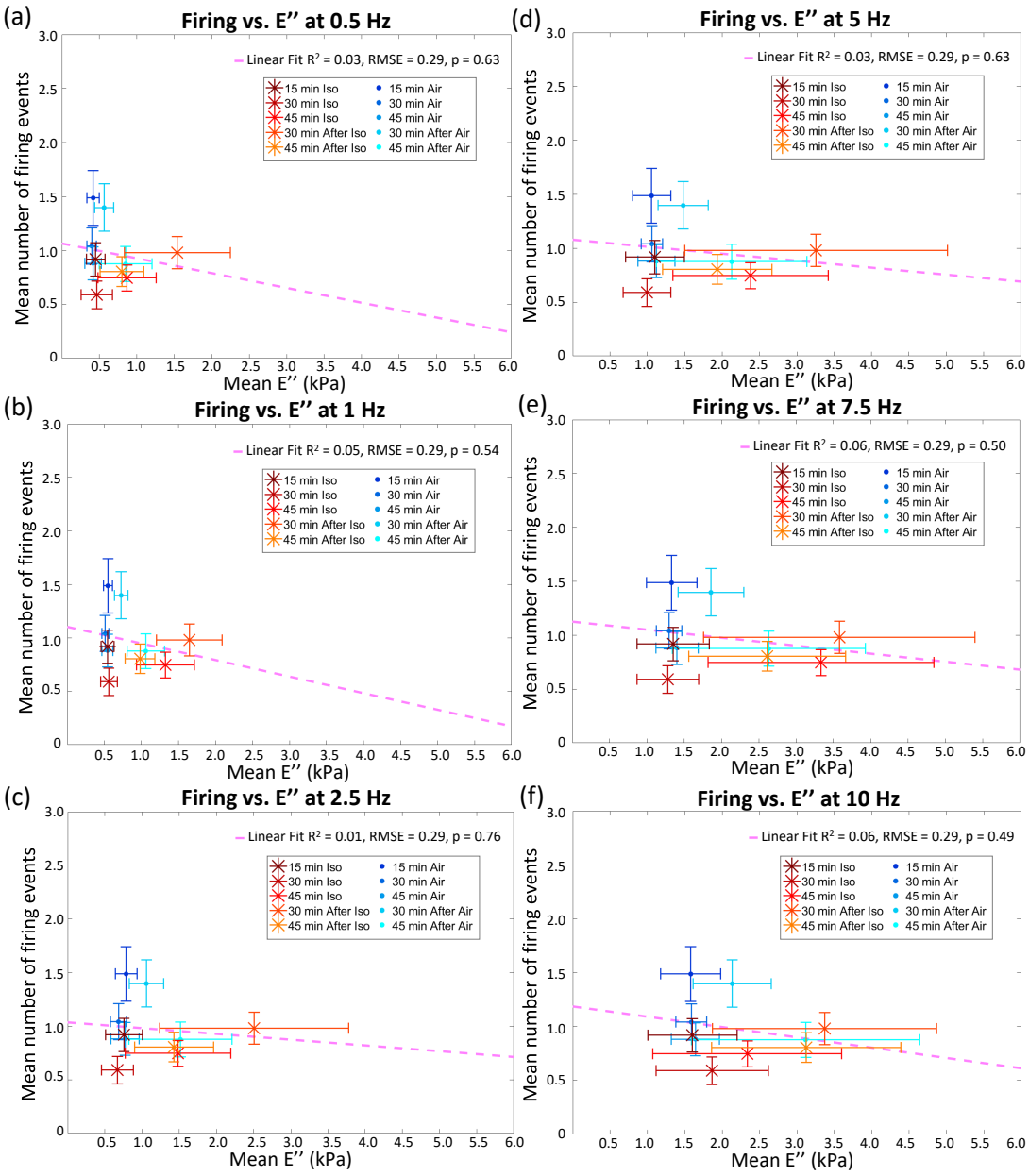

Figure S10: Correlation between neuronal firing and loss modulus. Neurons were treated with isoflurane (iso, red/yellow asterisk), or flowing air (air, blue/cyan points) as a control to determine effects caused by isoflurane. Linear regression (pink dashed lines, metrics shown in each panel and in Supplementary Table S14) was performed on the mean number of times neurons fired vs. mean neuronal loss modulus (E'') measured at: 0.5, 1, 2.5, 5, 7.5, or 10 Hz, shown in (a)-(f), respectively. Linear regression was performed on measurements collected at five experimental time points: 15, 30, and 45 min during gas exposure, and 30 and 45 min after gas exposure (indicated by point shading). Measurements before gas exposure were excluded because the sample was at a higher temperature during Before measurements than during subsequent measurements. Similarly, control measurements of no gas flow were excluded from the regression in order to avoid convoluting the effects of isoflurane with gas flow.

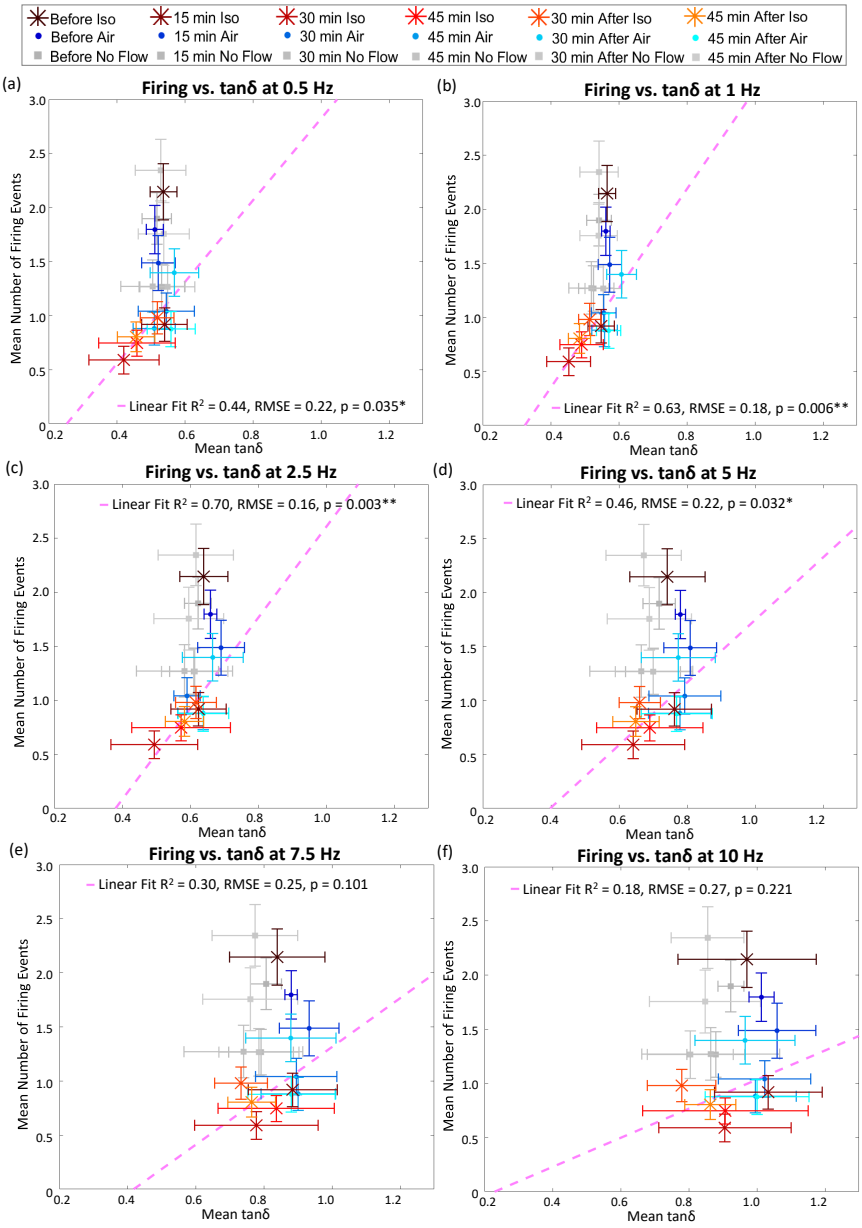

Figure S11: Correlation between neuronal firing and loss tangent with all data points. Neurons were treated with isoflurane (iso, asterisks), flowing air to control for the effects of the isoflurane (air, points), or no gas flow to control for the effects of gas flow through the experimental system (no flow, squares). Neuronal firing or loss tangent ($\tan\delta$) were measured at six experimental time points: before, 15, 30, and 45 min during, and 30 and 45 min after exposure to isoflurane (indicated by point shading, where Before is darkest and 45 min After is lightest). Points represent the mean number of times neurons fired vs. mean neuronal $\tan\delta$ at: 0.5, 1, 2.5, 5, 7.5, or 10 Hz, in (a)-(f), respectively. Linear regression (pink dashed lines) metrics are also shown in each panel and in Supplementary Table S14. Though all points are shown in this figure, regression was only performed on iso and flowing air control measurements at the during and after time points. Significant correlations are indicated by: * for $p < 0.05$ and ** for $p < 0.005$.

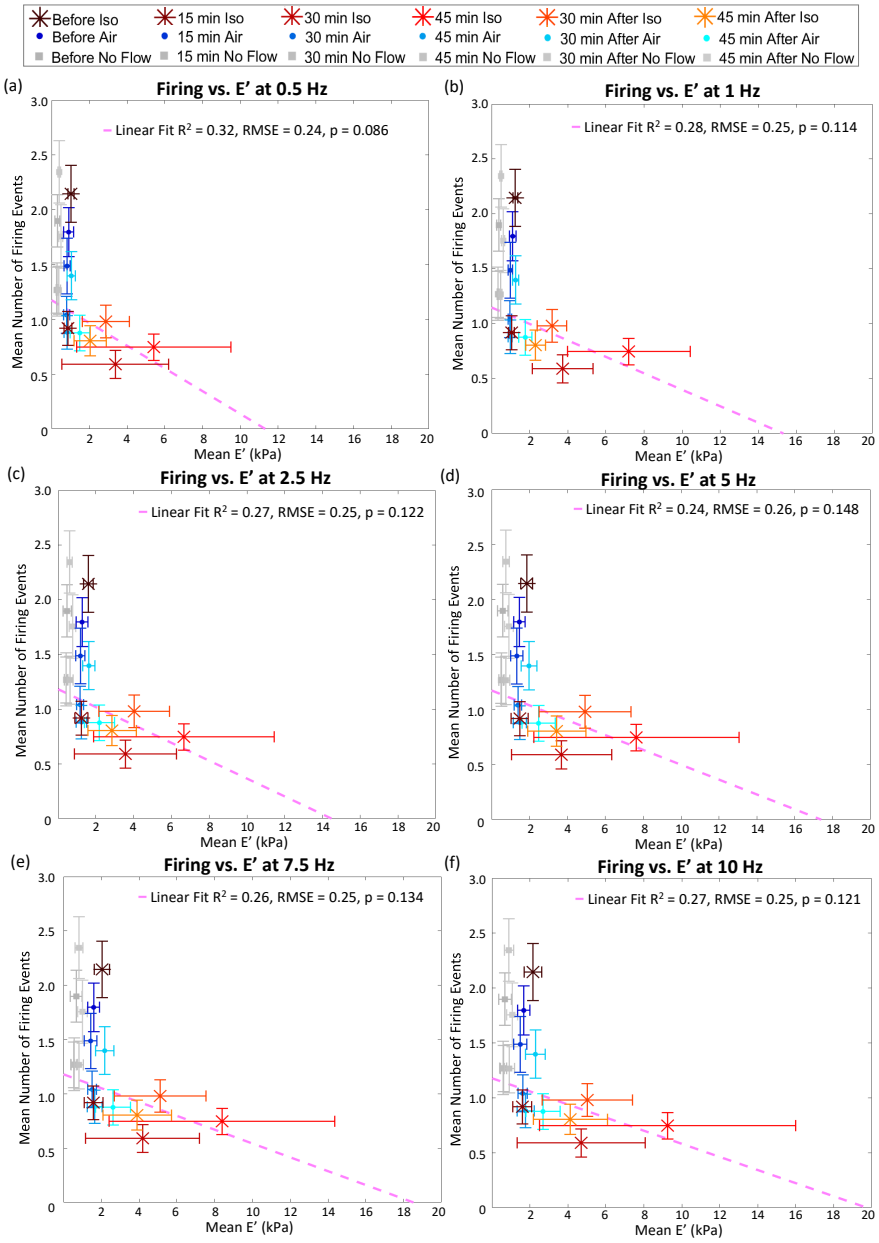

Figure S12: Correlation between neuronal firing and storage modulus with all data points. Neurons were treated with isoflurane (iso, asterisks), flowing air to control for the effects of the isoflurane (air, points), or no gas flow to control for the effects of gas flow through the experimental system (no flow, squares). Neuronal firing or storage modulus (E') were measured at six experimental time points: before, 15, 30, and 45 min during, and 30 and 45 min after exposure to isoflurane (indicated by point shading, where Before is darkest and 45 min After is lightest). Points represent the mean number of times neurons fired vs. mean neuronal E' at: 0.5, 1, 2.5, 5, 7.5, or 10 Hz, in (a)-(f), respectively. Linear regression (pink dashed lines) metrics are also shown in each panel and in Supplementary Table S14. Though all points are shown in this figure, regression was only performed on iso and flowing air control measurements at the during and after time points.

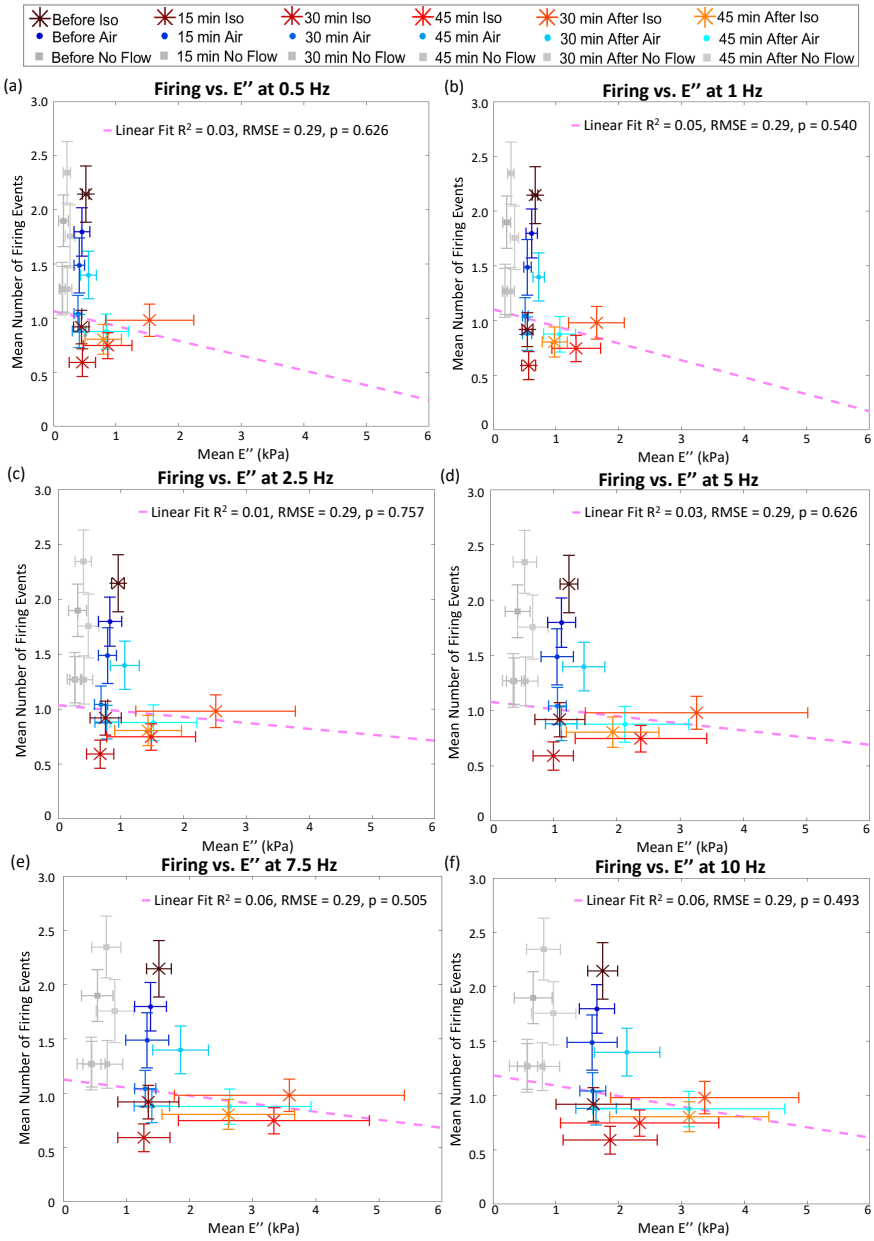

Figure S13: Correlation between neuronal firing and loss modulus with all data points. Neurons were treated with isoflurane (iso, asterisks), flowing air to control for the effects of the isoflurane (air, points), or no gas flow to control for the effects of gas flow through the experimental system (no flow, squares). Neuronal firing or loss modulus (E'') were measured at six experimental time points: before, 15, 30, and 45 min during, and 30 and 45 min after exposure to isoflurane (indicated by point shading, where Before is darkest and 45 min After is lightest). Points represent the mean number of times neurons fired vs. mean neuronal E'' at: 0.5, 1, 2.5, 5, 7.5, or 10 Hz, in (a)-(f), respectively. Linear regression (pink dashed lines) metrics are also shown in each panel and in Supplementary Table S14. Though all points are shown in this figure, regression was only performed on iso and flowing air control measurements at the during and after time points.

5 Supplementary Tables

Table S1: Unpaired t-test p-values comparing the storage modulus (E'), loss modulus (E''), and loss tangent ($\tan\delta$) of neurons with and without Oregon Green BAPTA. Oregon Green BAPTA is the fluorescence dye used in calcium imaging, and enters and fills the neuronal cytoplasm. Measurements were collected from 12 neurons with and 12 neurons without the dye, resulting in n=12 biologically independent samples. No significant differences exist in cell mechanics with and without the dye.

Frequency	E'	E''	$\tan\delta$
0.5 Hz	0.58	0.97	0.34
1 Hz	0.47	0.98	0.26
2.5 Hz	0.66	0.86	0.59
5 Hz	0.69	0.88	0.90
7.5 Hz	0.74	0.86	0.63
10 Hz	0.75	0.94	0.26

Table S2: Wilcoxon rank sum test p-values comparing the fraction of neurons that fire in different treatments. Cells were treated with a flow of isoflurane gas (iso, n=10 biologically independent samples, 184 cells total), a flowing air control (air, n=8 biologically independent samples, 169 cells total), or a control of room air without any gas flow (no flow, n=6 biologically independent samples, 151 cells total). Significant differences are indicated by: * for $p < 0.05$, ** for $p < 0.005$, and *** for $p < 0.0001$.

Time point	Iso vs. Air	Iso vs. No Flow	Air vs. No Flow
Before	0.76	0.09	0.11
15 min During	0.63	* 0.016	0.059
30 min During	* 0.03	** 0.001	0.059
45 min During	0.97	* 0.012	* 0.029
30 min After	0.71	** 0.003	** 0.0027
45 min After	0.85	* 0.042	* 0.013

Table S3: Wilcoxon rank sum test p-values comparing neuron firing counts in different treatments. Cells were treated with a flow of isoflurane gas (iso, n=10 biologically independent samples, 184 cells total), a flowing air control (air, n=8 biologically independent samples, 169 cells total), or a control of room air without any gas flow (no flow, n=6 biologically independent samples, 151 cells total). Significant differences are indicated by: * for $p < 0.05$, ** for $p < 0.005$, and *** for $p < 0.0001$.

Time point	Iso vs. Air	Iso vs. No Flow	Air vs. No Flow
Before	0.55	0.83	0.73
15 min During	0.20	0.13	0.80
30 min During	** 0.0014	** 0.0043	0.84
45 min During	0.50	0.31	0.73
30 min After	0.30	*** 0.0001	** 0.0055
45 min After	0.80	* 0.014	* 0.01

Table S4: Wilcoxon rank sum test p-values comparing changes in neuron firing counts through time. Cells were treated with a flow of isoflurane gas (iso, n=10 biologically independent samples, 184 cells total), a flowing air control (air, n=8 biologically independent samples, 169 cells total), or a control of room air without any gas flow (no flow, n=6 biologically independent samples, 151 cells total). Significant differences are indicated by: * for $p < 0.05$, ** for $p < 0.005$, and *** for $p < 0.0001$.

Comparison	Iso	Air	No Flow
15 min During vs. Before	*** 0.00	* 0.015	* 0.017
30 min During vs. 15 min During	* 0.011	0.60	0.36
45 min During vs. 30 min During	* 0.045	0.57	0.99
30 min After vs. 45 min During	0.59	0.37	** 0.0016
45 min After vs. 30 min After	0.36	* 0.04	* 0.023

Table S5: Unpaired t-test p-values comparing the fraction of neurons that reactivated during a specific time point in each treatment. Cells were treated with a flow of isoflurane gas (iso, n=10 biologically independent samples, 184 cells total), a flowing air control (air, n=8 biologically independent samples, 169 cells total), or a control of room air without any gas flow (no flow, n=6 biologically independent samples, 151 cells total). Significant differences are indicated by: * for $p < 0.05$, ** for $p < 0.005$, and *** for $p < 0.0001$.

Time point	Iso vs. Air	Iso vs. No Flow	Air vs. No Flow
30 min During	0.61	0.82	0.80
45 min During	* 0.038	0.14	0.57
30 min After	0.97	0.87	0.85
45 min After	* 0.022	0.85	0.07

Table S6: Unpaired t-test p-values comparing the fraction of cells that activated between specific time points. Cells were treated with a flow of isoflurane gas (iso, n=10 biologically independent samples, 184 cells total), a flowing air control (air, n=8 biologically independent samples, 169 cells total), or a control of room air without any gas flow (no flow, n=6 biologically independent samples, 151 cells total). Significant differences are indicated by: * for $p < 0.05$, ** for $p < 0.005$, and *** for $p < 0.0001$.

Time point	Iso	Air	No Flow
30 min During vs. 15 min During	0.15	1.00	0.54
45 min During vs. 30 min During	* 0.026	0.90	0.79
30 min After vs. 45 min During	0.65	0.93	* 0.047
45 min After vs. 30 min After	0.90	0.08	0.067

Table S7: Unpaired t-test p-values comparing the fraction of cells that inactivated between specific time points. Cells were treated with a flow of isoflurane gas (iso, n=10 biologically independent samples, 184 cells total), a flowing air control (air, n=8 biologically independent samples, 169 cells total), or a control of room air without any gas flow (no flow, n=6 biologically independent samples, 151 cells total). Significant differences are indicated by: * for $p < 0.05$, ** for $p < 0.005$, and *** for $p < 0.0001$.

Time point	Iso	Air	No Flow
30 min During vs. 15 min During	* 0.031	0.060	0.86
45 min During vs. 30 min During	* 0.030	0.63	0.08
30 min After vs. 45 min During	* 0.050	0.91	0.15
45 min After vs. 30 min After	0.36	0.67	* 0.040

Table S8: Unpaired t-test p-values comparing the fraction of neurons that activated (started firing) at a specific time point between treatments. Cells were treated with a flow of isoflurane gas (iso, n=10 biologically independent samples, 184 cells total), a flowing air control (air, n=8 biologically independent samples, 169 cells total), or a control of room air without any gas flow (no flow, n=6 biologically independent samples, 151 cells total). Significant differences are indicated by: * for $p < 0.05$, ** for $p < 0.005$, and *** for $p < 0.0001$.

Time point	Iso vs. Air	Iso vs. No Flow	Air vs. No Flow
15 min During	0.89	0.87	0.80
30 min During	0.22	0.19	0.93
45 min During	0.43	0.22	0.72
30 min After	0.71	0.22	0.15
45 min After	0.09	0.58	0.21

Table S9: Unpaired t-test p-values comparing the fraction of neurons that inactivated (stopped firing) at a specific time point between treatments. Cells were treated with a flow of isoflurane gas (iso, n=10 biologically independent samples, 184 cells total), a flowing air control (air, n=8 biologically independent samples, 169 cells total), or a control of room air without any gas flow (no flow, n=6 biologically independent samples, 151 cells total). Significant differences are indicated by: * for $p < 0.05$, ** for $p < 0.005$, and *** for $p < 0.0001$.

Time point	Iso vs. Air	Iso vs. No Flow	Air vs. No Flow
15 min During	0.33	0.054	0.24
30 min During	0.28	0.97	0.30
45 min During	0.15	0.40	0.50
30 min After	0.44	0.07	0.25
45 min After	0.54	0.58	0.30

Table S10: Unpaired t-test p-values comparing changes in neuron reactivation (where a neuron started firing again after having fired then inactivated in previous time points) through time. Cells were treated with a flow of isoflurane gas (iso, n=10 biologically independent samples, 184 cells total), a flowing air control (air, n=8 biologically independent samples, 169 cells total), or a control of room air without any gas flow (no flow, n=6 biologically independent samples, 151 cells total). Significant differences are indicated by: * for $p < 0.05$, ** for $p < 0.005$, and *** for $p < 0.0001$.

Time Point Comparison	Iso	Air	No Flow
45 min During vs. 30 min During	0.09	0.76	0.96
30 min After vs. 45 min During	0.35	0.24	0.24
45 min After vs. 30 min After	0.90	0.06	0.88

Table S11: Multi-factorial analysis of variance (ANOVA) results for neuron storage modulus (E'), loss modulus (E''), and loss tangent ($\tan\delta$) measurements at six different frequencies throughout six different time points during treatment exposure. Treatments were isoflurane gas (n=5 independent samples/cells), flowing air (n=5 independent samples/cells), and air without any gas flow (n=3 independent samples/cells) Significant differences are indicated by: * for $p < 0.05$, ** for $p < 0.005$, and *** for $p < 0.0001$.

Variable	ANOVA p-value		
	E'	E''	$\tan\delta$
Frequency	0.37	*** 0	*** 0
Treatment	*** 0	*** 0	** 0.0002
Time Point	** 0.0025	*** 0	0.43
Frequency and Treatment	1.00	0.35	0.92
Frequency and Time Point	1.00	1.00	1.00
Treatment and Time Point	*** 0	** 0.0007	0.86

Table S12: Significant differences in neuron storage modulus (E'), loss modulus (E''), and loss tangent ($\tan\delta$) between experimental treatments, determined by *post hoc* application of Tukey's honest significant difference criterion. Neurons were treated with a flow of isoflurane gas (iso, n=5 independent samples/cells), a flowing air control (air, n=5 independent samples/cells), or a control of room air without any gas flow (no flow, n=3 independent samples/cells). Significant differences are indicated by: * for $p < 0.05$, ** for $p < 0.005$, and *** for $p < 0.0001$.

Comparison	E' p-value	E'' p-value	$\tan\delta$ p-value
Iso 45 min during vs. Air 45 min during	*** 7.00e-7	* 0.035	0.98
Iso 30 min after vs. Air 30 min after	0.21	*** 8.7e-5	0.57
Iso 30 min after vs. No Flow 30 min after	0.061	*** 7.07e-7	1.00
Iso 45 min after vs. No Flow 45 min after	0.71	* 0.018	1.00
Iso 45 min during vs. No Flow 45 min during	*** 7.01e-7	** 0.00062	1.00
Air 45 min after vs. No Flow 45 min after	0.99	* 0.0068	1.00

Table S13: Significant differences in neuron storage modulus (E'), loss modulus (E''), and loss tangent ($\tan\delta$) between experimental time points, determined by *post hoc* application of Tukey's honest significant difference criterion. Neurons were treated with a flow of isoflurane gas (iso, n=5 independent samples/cells), a flowing air control (air, n=5 independent samples/cells), or a control of room air without any gas flow (no flow, n=3 independent samples/cells). Significance is indicated by: * for $p < 0.05$, ** for $p < 0.005$, and *** for $p < 0.0001$.

Isoflurane			
Comparison	E' p-value	E'' p-value	$\tan\delta$ p-value
Iso before vs. Iso 45 min during	*** 7e-7	0.13	1.00
Iso before vs. Iso 30 min after	0.18	*** 2.45e-6	0.95
Iso 15 min during vs. Iso 45 min during	*** 1.00e-7	* 0.042	0.98
Iso 15 min during vs. Iso 30 min after	0.094	*** 1.08e-6	0.87
Iso 30 min during vs. Iso 45 min during	** 0.0042	* 0.045	1.00
Iso 30 min during vs. Iso 30 min after	1.00	*** 1.15e-6	1.00
Iso 45 min during vs. Iso 30 min after	* 0.01	0.60	1.00
Iso 45 min during vs. Iso 45 min after	*** 3.63e-5	1.00	1.00
Air Control			
Comparison	E' p value	E'' p value	$\tan\delta$ p value
Air 15 min during vs. Air 45 min after	1.00	* 0.046	1.00

Table S14: Linear regression results for correlation between the mean number of times neurons fire and mean neuronal storage modulus (E'), loss modulus (E''), or loss tangent ($\tan\delta$) at each measurement frequency. Regression details are provided in the statistics section of Materials and Methods. Regression R^2 values, root mean square errors (RMSE), and p-values are shown. Significant correlations are indicated by: * for $p < 0.05$ and ** for $p < 0.005$.

	E' (Pa)			E'' (Pa)			$\tan\delta$		
Frequency (Hz)	R^2	RMSE	p-Value	R^2	RMSE	p-Value	R^2	RMSE	p-Value
0.5	0.32	0.24	0.09	0.03	0.29	0.63	0.44	0.22	* 0.04
1	0.28	0.25	0.11	0.05	0.29	0.54	0.63	0.18	* 0.01
2.5	0.27	0.25	0.12	0.01	0.29	0.76	0.70	0.16	** 0.0027
5	0.24	0.26	0.15	0.03	0.29	0.63	0.46	0.22	* 0.03
7.5	0.26	0.25	0.13	0.06	0.29	0.50	0.30	0.25	0.10
10	0.27	0.25	0.12	0.06	0.29	0.49	0.18	0.27	0.22

Supplementary References

[1] Luca Bartolini, Davide Iannuzzi, and Giorgio Mattei. Comparison of frequency and strain-rate domain mechanical characterization. *Scientific Reports*, 8(1):13697, December 2018.

[2] Nikolai Born. *User Manual: Chiaro Nanoindenter*. Optics11.

[3] G Gruca, S de Man, M Slaman, J H Rector, and D Iannuzzi. Ferrule-top micromachined devices: design, fabrication, performance. *Measurement Science and Technology*, 21(9):094033, September 2010.

[4] Francis T.S Yu and Paul B Shizhuo Yin, Ruffin. *Fiber optic sensors*. CRC press, Boca Raton; London; New York, 2008. OCLC: 494403019.

[5] D. Rugar, H. J. Mamin, and P. Guethner. Improved fiber-optic interferometer for atomic force microscopy. *Applied Physics Letters*, 55(25):2588–2590, December 1989.